JOURNAL OF MATERIALS SCIENCE **35** (2000) 2719–2727

Comparison of tensile properties in the pre-yield region of metallocene-catalyzed and Ziegler-Natta-catalyzed linear polyethylenes

K. NITTA*, K. SUZUKI
School of Materials Science, Japan Advanced Institute of Science and Technology (JAIST), 923-1292 Japan
E-mail: nitta@jaist.ac.jp

A. TANAKA
Department of Materials Science, The University of Shiga Prefecture, 2500, Hassaka, Hikone, Shiga 522-8533 Japan

The mechanical nonlinear behaviour of metallocene- and Ziegler-Natta catalyzed polyethylenes with various contents of short chain branching was investigated using a nonlinear constitutive equation in which the plastic deformation and the anharmonicity of elastic response are taken into account. It is suggested that the mechanical behaviour is governed by the plastic deformation for the Ziegler-Natta catalyzed polyethylenes, whereas the anharmonicity strongly affects the mechanical behaviour for metallocene-catalyzed polyethylenes.

1. Introduction

In recent years, much attention has been focused on the mechanical properties such as toughness and stiffness for polyethylene solids because of the growing use in engineering applications such as water and gas pipes [1–3]. For the materials design, a simple mathematical model for predicting mechanical responses under loading and deformation, particularly in the pre-yield region, is desirable [4]. It has been identified, however, that the mechanical properties of polyethylene (PE) materials are highly nonlinear and time-dependent so that the use of linear viscoelastic theory for PE is limited to the prediction of mechanical response even at small deformations [5]. This is because PE materials exhibit viscoelasticity accompanying the elastic anharmonicity [6–8] and plastic deformation [9–11]. To characterize such complex behaviour, we have developed a constitutive model that describes nonlinear viscoelastic behaviour accompanying the anharmonicity in elastic response and plastic deformation [12].

In the past, linear polyethylenes and related copolymers synthesized using Ziegler-Natta catalysts have been widely studied [13–17]. However, much important information is of limited utility in understanding the general characteristics of the mechanical properties of polyethylenes. The reason for this situation lies in the polydispersity in composition and in molecular weight, which is a typical feature of the conventional polyethylenes used in the past [18–20]. The development of the single-site metallocene catalysts [21] has led to a new type of linear polyethylene having narrower molecular weight distribution and homogeneous comonomer distribution [22, 23]. Thus, the microstructure of the metallocene-catalyzed polyethylenes differs significantly from that of Ziegler-Natta-catalyzed polyethylenes.

In this work, we have studied the mechanical nonlinearity of metallocene-catalyzed polyethylenes which contain various degrees of short-chain branching, in comparison with the corresponding Ziegler-Natta catalyzed linear polyethylenes. A nonlinear viscoelastic model including two nonlinear factors of the plastic deformation and the anharmonic elasticity was used to analyze the mechanical data. Moreover, the resulting predictions in stress relaxation were compared with the experimental relaxation data and the applicability of the constitutive equation was examined. The final objective of the present work is to provide the constitutive equation suitable for mechanical response in the pre-yield regions of polyethylene solids.

2. Theoretical survey

In the previous article [12], a nonlinear constitutive equation was developed by introducing anharmonic springs and the plastic strain component into the linear viscoelastic model. Details of these theoretical processes and the analytical procedure are presented in the previous study. Here we briefly repeat its main outline.

* Author to whom all correspondence should be addressed.

According to the linear viscoelastic theory [24], the constitutive relation is given by the following integral form:

$$\sigma(t) = \int_{-\infty}^{t} E(t-t')\left(\frac{\mathrm{d}\varepsilon}{\mathrm{d}t'}\right)\mathrm{d}t' \qquad (1)$$

where $\sigma(t)$ is the true stress as a function of time t, ε is the natural strain, and $E(t)$ is known as the relaxation modulus for the material which is given by

$$E(t) = \int_{-\infty}^{\infty} H(\tau)\exp\left(-\frac{t}{\tau}\right)\mathrm{d}\ln\tau \qquad (2)$$

where τ is the relaxation time and $H(\tau)$ is the spectrum of relaxation times expressed as a function of $\ln\tau$. Here, the anharmonicity in elastic response is introduced into the above viscoelastic model. The nonlinear elastic element with an anharmonic potential function proposed by Toda [25] is employed on the basis of the previous idea. After some algebraic manipulations, one obtains the stress response to an arbitrary strain input:

$$\sigma(t) = \int_{-\infty}^{t} E(t-t';\varepsilon)\left(\frac{\mathrm{d}\varepsilon}{\mathrm{d}t'}\right)\mathrm{d}t' \qquad (3)$$

and the response function $E(t;\varepsilon)$ has the form:

$$E(t;\varepsilon) = \int_{-\infty}^{\infty} H(\tau)\frac{e^{-t/\tau}e^{-2\gamma_G\varepsilon}}{[1-(1-e^{-2\gamma_G\varepsilon})(1-e^{-t/\tau})]^2}\mathrm{d}\ln\tau \qquad (4)$$

where γ_G is a nonlinear parameter which expresses the anharmonicity of elastic response. The nonlinear parameter γ_G corresponds to the Grüneisen constant which can be estimated by $-\mathrm{d}\ln\sqrt{E}/\mathrm{d}\varepsilon$ [26, 27]. If the applied strain is small, the denominator of Equation 4 is approximately equal to unity so that the response function $E(t;\varepsilon)$ is separable into the strain dependent term $\Gamma(\varepsilon)$ and the time-dependent term $E(t)$ as follows:

$$E(t;\varepsilon) = E(t)\Gamma(\varepsilon) \qquad (5)$$

where $E(t)$ is given by Equation 2 and the anharmonic function $\Gamma(\varepsilon)$ becomes the exponential decay function as follows:

$$\Gamma(\varepsilon) = \exp(-2\gamma_G\varepsilon) \qquad (6)$$

Such separable form of the response function has been verified in typical semicrystalline solids by previous experimental studies [28–31].

In view of the plasto-viscoelastic behaviour, we assume that the plastic deformation induces overestimation of the strain. Therefore, a part of the applied strain is consumed as plastic deformation and the remainder contributes effectively to the generation of the stress. Hence, we introduce the effective strain fraction $\Psi(t)$, which can be defined as the contribution of the effective strain to the total strain γ:

$$\mathrm{d}\varepsilon = \Psi(t)\,\mathrm{d}\gamma = \left(\frac{\mathrm{d}\gamma}{\mathrm{d}t}\right)\Psi(t)\,\mathrm{d}t \qquad (7)$$

Hereafter the strain ε is referred to as the effective strain and the γ as the applied strain. Considering that a material is deformed at a constant rate and the deformation is applied at $t = 0$, the strain γ can be approximated by $\ln(1 + Rt)$ where R is the nominal-stain rate. Then we obtain

$$\sigma(t) = \int_{0}^{t} E(t-t')\Gamma(\varepsilon)\frac{R}{1+Rt'}\Psi(t')\,\mathrm{d}t' \qquad (8)$$

3. Experimental

3.1. Materials and sample preparation

In this work, two sets of linear polyethylenes covering an ethylene-1-hexene comonomer content of 0 to 3.5 mol% were used. One is a new type of polyethylene prepared using a metallocene catalyst system and the other one is a conventional type of polyethylene prepared using a Ziegler-Natta catalyst.

The molecular characteristics of all the samples are given in Table I. The weight and number average molecular weights were obtained from gel permeation chromatography by following conventional procedures. The co-unit content was determined by high-resolution ^{13}C NMR using established methods and assignments that are reported in the literature [32, 33]. All the polymers have approximately the same molecular weight but the metallocene-catalyzed polyethylenes have a narrower distribution (M_w/M_n close to 2). The nomenclature used in this study is as follows: M-PE is the metallocene-catalyzed polyethylene, ZN-PE the Ziegler-Natta catalyzed polyethylenes, and its end numeral the average content of short chain branching (SCB) in mol%.

According to temperature rising elution fractionation (TREF) measurements [34], the M-PE polymers show homogeneous composition whereas the ZN-PE polymers are composed of three fractions in which the first fraction with a higher molecular weight has little SCB content, the second one is the main component with the average degree of SCB and the average molecular weight, and the third one is the component having a higher SCB and a lower molecular weight.

TABLE I Molecular characteristics of samples

Sample	M_w (10^4)	M_n (10^4)	M_w/M_n	SCB/mol %
M-PE0	6.70	3.00	2.23	0
M-PE0.9	7.80	4.40	1.77	0.88
M-PE1.8	7.90	4.60	1.72	1.82
M-PE2.2	7.40	4.10	1.80	2.18
M-PE3.1	8.00	4.80	1.67	3.08
M-PE3.5	7.70	4.30	1.79	3.54
ZN-PE0	5.80	1.19	4.87	0
ZN-PE0.9	8.70	2.80	3.11	0.92
ZN-PE2.5	8.40	2.70	3.11	2.52
ZN-PE3.4	9.00	2.80	3.21	3.42

These polyethylenes were melt pressed in a laboratory press at 463 K and at 10 MPa for 3 min. Samples quenched at 273 K were prepared for the measurements. The thickness of the compression molded samples was adjusted to suit the intended experiment.

3.2. Sample characterization

The densities for all samples were measured at 303 K using the floatation method. Binary media prepared from various ratios of distilled water and ethyl alcohol were used. The degrees of crystallinity were calculated from a relationship with constants of 1000 and 856 kg/m^3 for the density of the crystalline and amorphous regions, respectively [35].

The small angle X-ray scattering (SAXS) measurement was performed with point focusing optics and an one-dimensional position sensitive proportional counter (PSPC) with an effective length of 100 mm. The SAXS optics has a toroidal mirror and a crystal monochromator to focus the scattered intensity on the PSPC. The Cu K_α radiation supplied by a MAC Science M18X generator operating at 40 kV and 30 mA was used throughout. The distance between the sample and PSPC was about 0.4 m. The geometry was further checked by a chicken tendon collagen sample, which gives a set of sharp diffractions corresponding to a period of 65.3 nm.

From the volume fraction crystallinity χ_v obtained from the density data and the SAXS long period L_p, the lamellar crystal thickness L_c and the amorphous layer thickness L_a can be determined from the following relationships: $L_c = \chi_v L_p$ and $L_a = (1 - \chi_v)L_p$.

As is seen in Fig. 1, the introduction of noncrystallizing co-unts into the main chain leads to a continuous decrease in the lamellar thickness with increasing SCB content. It is interesting to note that the lamellar thickness of M-PEs is lower that that of ZN-PE at the same SCB content and the amorphous layer thickness of M-PE remains constant. This is because the methylene stem length that is crystallizable is effectively reduced by the homogeneous introduction of α-olefin units. It should be noted here that an important difference in lamellar morphology between both PEs is that ZN-PE has a greater heterogeneity in lamellar and amorphous layer thicknesses.

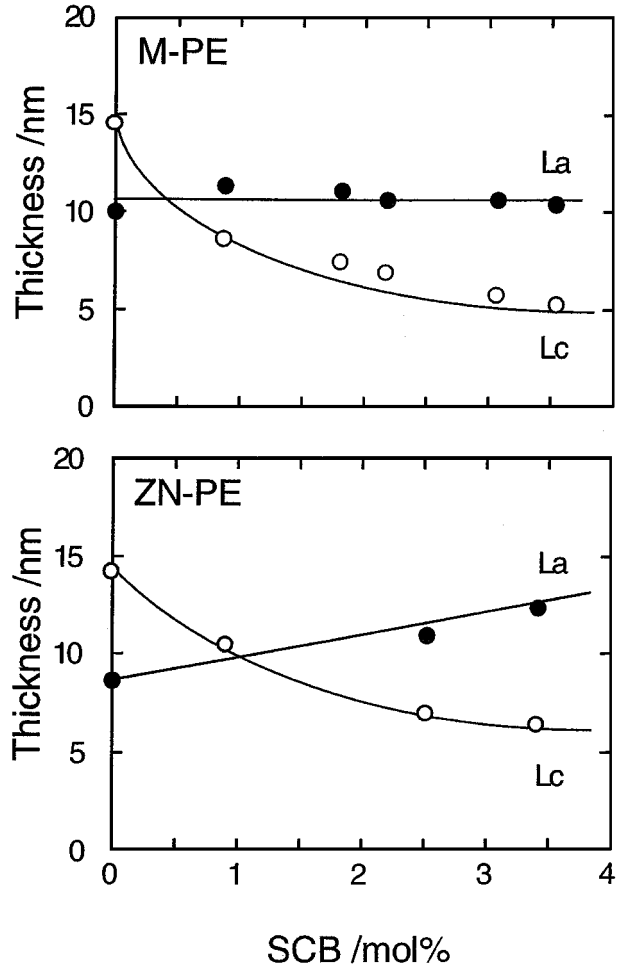

Figure 1 SCB dependences of crystalline thickness (○) and amorphous layer thickness (●) for metallocene-catalyzed PEs and Ziegler-Natta-catalyzed PEs.

3.3. Measurements

3.3.1. Analytical method

In this section, an analytical method for determining the mechanical parameters such as the Grüneisen constant and the plastic deformation fraction is presented. Considering that the oscillatory modulus $E^*(\omega)$ can be given by $\mathcal{F}[E(t)]/i\omega$, where $i = \sqrt{-1}$, ω is the angular frequency and the operator $\mathcal{F}$ denotes the Fourier transformation. The Fourier transformation of the nonlinear response function $E(t;\varepsilon)$ has the form:

$$\mathcal{F}[E(t;\varepsilon)] = \mathcal{F}[E(t)]\Gamma(\varepsilon) = (i\omega)^{-1}E^*(\omega)\Gamma(\varepsilon) \quad (9)$$

Thus, the anharmonic function $\Gamma(\varepsilon)$ at any elongation time t can be obtained by the transient dynamic moduli data during elongation:

$$\Gamma(\varepsilon)|_{t=t} = \frac{|E^*(\omega)|_{t=t}}{|E^*(\omega)|_{t=0}} \quad (10)$$

Also, using the Laplace transformation of the nonlinear constitutive Equation 8, one can obtain the solution for the transient effective strain fraction $\Psi(t)$ as follows:

$$\Psi(t) = \frac{1+Rt}{R}\mathcal{L}^{-1}\left[\frac{\mathcal{L}[\sigma(t)]}{\mathcal{L}[E(t;\varepsilon)]}\right] \quad (11)$$

where the operator $\mathcal{L}$ denotes the Laplace transform. The value of the response function $E(t;\varepsilon)$ at any elongation time t can be determined from the linear relaxation modulus data $E(t)$ and the anharmonic function $\Gamma(\varepsilon)$ at any time evaluated from Equation 10. Substituting the values of $E(t;\varepsilon)$ and the stress $\sigma(t)$ at any time into Equation 11 gives the value of the effective strain fraction $\Psi(t)$ as a function of time. Subsequently, the effective strain ε at any time t can be calculated using

$$\varepsilon|_{t=t} = \frac{R}{1+Rt}\int_0^t \Psi(t')\,dt' \quad (12)$$

Combination of Equations 10 and 12 gives the relationship between the anharmonic function and the effective

strain, and the Grüneisen constant can be obtained from the slope of the ln $\Gamma(\varepsilon)$ vs. ε relation:

$$\gamma_G = -\frac{1}{2}\frac{d\ln\Gamma(\varepsilon)}{d\varepsilon} \quad (13)$$

Furthermore, the transient plastic deformation fraction $\phi_{PL}(t)$ can be determined by the following equation:

$$\phi_{PL}(t) = \frac{\gamma - \varepsilon}{\gamma} = 1 - \frac{1}{\gamma}\int_0^t \dot{\gamma}\,\Psi(t')\,dt' \quad (14)$$

where $\phi_{PL}(t)$ indicates the accumulated plastic strains when current deformation is applied.

In summary, the measurements of stress and strain under simultaneous elongation and oscillation make it possible to quantitatively determine the differences between the variation of transient moduli during elongation and the derivative curve of the stress-strain relation. Thus the horizontal shifts for the derivative curve of the stress-strain relation are necessarily in agreement with the values obtained from the simultaneous measurements. The horizontal shifts provide the effective strain fraction; moreover, the anharmonicity in elastic response can be evaluated from the changes in the transient modulus with respect to the effective strain.

3.3.2. Experimental method

The determination for the nonlinear parameters such as the plastic deformation fraction and the Grüneisen constant demands the measurement of the transient modulus data during an uniaxial elongation at a constant rate of deformation. A dynamic mechanical analyzer (Rheology Co., Ltd. DVE V-4) was modified to have the capability of subjecting a film specimen to a constant-rate elongation together with small-amplitude sinusoidal strain. The elongational rate was 1.0 mm/min ($R = 0.0833\%$/s), the initial length between the clamps was 20 mm, the amplitude of oscillatory deformation was 10 μm, and the frequency of the oscillation was 100 Hz. The experimental setup is illustrated in Fig. 2.

When a sinusoidal strain superimposed onto an elongation strain is applied to a specimen under the condition of $R \ll \omega/2\pi$, the stress response $\sigma(t)$ can

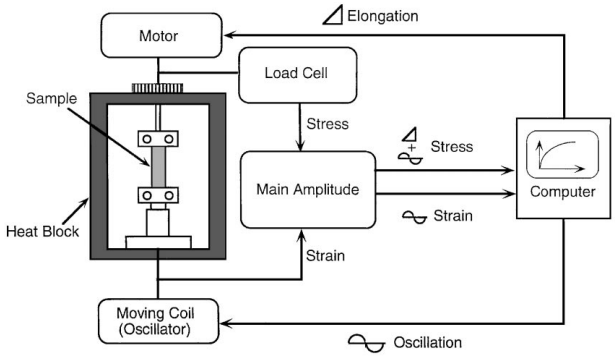

Figure 2 Schema of the experimental set-up for tensile measurement with a sinusoidal deformation.

be expressed by the fundamental components of the Fourier expansion:

$$\sigma^*(t) = \sigma(t) + a_1\exp(i\omega t) + b_1\exp(-i\omega t) \quad (15)$$

In this work, the transient modulus during elongation was defined as

$$|E^*(\omega)| = \frac{\sqrt{a_1^2 + b_1^2}}{\gamma_0} \quad (16)$$

The linear relaxation modulus $E(t)$ was evaluated from the master curves of linear dynamic moduli in the undeformed state using the following equation [36]:

$$E(t) = E'(\omega) - 0.560E''\left(\frac{\omega}{2}\right) + 0.200E''(\omega)|_{\omega=\frac{1}{t}} \quad (17)$$

The frequency dependence of the dynamic moduli was measured in the frequency range of 0.02 and 200 Hz at temperatures between 290 K and 353 K. The relaxation component of $E(t)$, and the relaxation spectrum $H(\tau)$ were also formulated by means of an analytical technique being referred to as "Procedure X" [37].

The Poisson ratios for all the samples were measured using an Instron Model-4466 in order to evaluate the true stress required for the analysis. The cross sectional area in the deformed portion was transiently measured as a function of strain. Also, the specimen was confirmed to be homogeneously deformed in the pre-yield regions, leading to the relation $\gamma = \ln(1 + Rt)$. Details of the experimental method were described in the previous paper [12].

4. Results and discussion

Fig. 3 shows the true stress vs. elongation time curves measured together with the oscillatory deformation for all the samples. It is confirmed (but not presented here) that the curves are identical with the curves without the oscillatory deformation. In this work, the curves in the pre-yield strain region, where all PE samples showed no stress-whitening or necking and are homogeneously deformed, are analyzed.

As seen in Fig. 3, lowering the SCB content causes the overall stress to decrease in this strain region. It should be noted here that M-PE samples show a greater effect of comonomer unit on the stress magnitude; moreover, the ZN-PE0, M-PE0, and ZN-PE0.9 samples exhibiting a relatively higher stress showed stress-whitening in the post-yield region.

4.1. Plastic deformation fraction

Fig. 4 shows the variation of the plastic deformation fraction ϕ_{PL} with elongation time t. As seen in the figures, ϕ_{PL} increases monotonically with elongation for all the samples and an increase in the SCB content lowers the magnitude of ϕ_{PL}. It is interesting to note that the magnitude of ϕ_{PL} at an applied strain $\gamma = 0.16$ (or elongation time = 200 s) for the ZN-PE is greater than that for M-PE, as is shown in Fig. 5. Furthermore, we

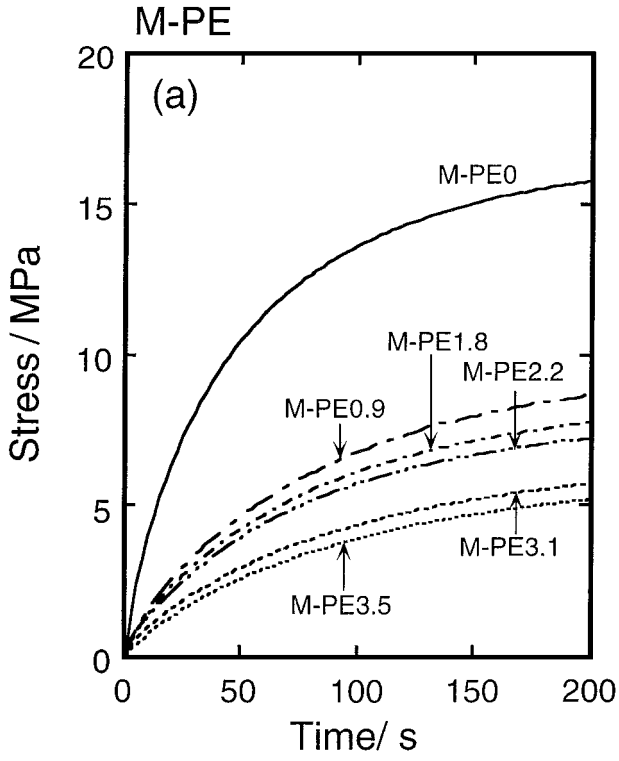

Figure 3 True stress-elongation time curves under a strain rate of 0.08%/s at 298 K for (a) metallocene-catalyzed PEs and (b) Ziegler-Natta-catalyzed PEs.

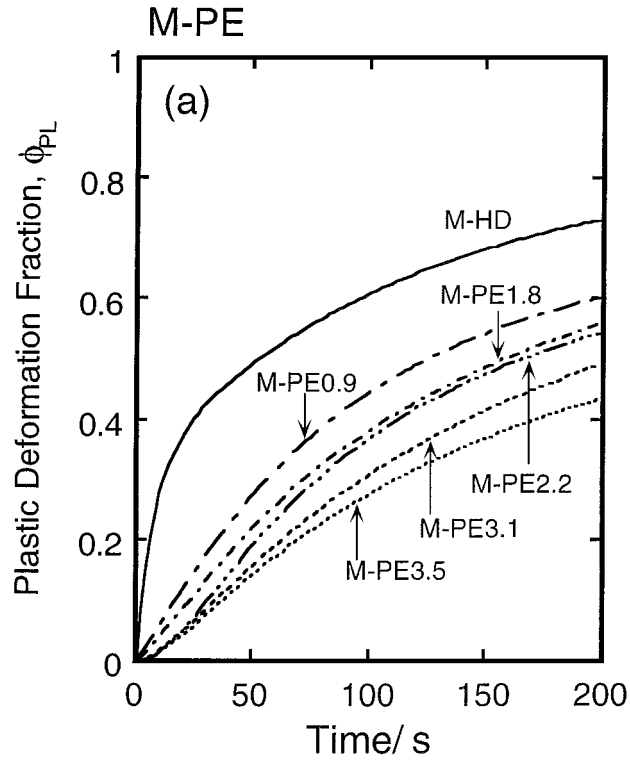

Figure 4 Plastic deformation fraction $\phi_{PL}(t)$ plotted against the elongational time under a strain rate of 0.08%/s at 298 K for (a) metallocene-catalyzed PEs and (b) Ziegler-Natta-catalyzed PEs.

found a linear relationship between the crystallinity and the plastic deformation fraction (see Fig. 6), indicating that the plastic deformation generated in the pre-yield region is governed by the crystal fraction. This is plausible since the plastic deformation occurs predominantly in the crystalline region [9, 10].

The derivative of ϕ_{PL} with respect to the elongation time are plotted against elongation time in Fig. 7. It was found that the derivative values of ϕ_{PL} show a maximum at smaller strains for all samples, suggesting that the plastic deformation occurs progressively in the initial strain region. In particular, M-PE0, ZN-PE0, and ZN-PE0.9 samples exhibit a sharp increase in $d\phi_{PL}/dt$ and showed stress-whitening in the higher strain regions; *i.e.* beyond yield point or necking region. These results suggest that in the case of higher density PEs, plastic deformation such as molecular-level cracks and microvoids generated from the structural flaws that occur in the initial strain region, which then develop into macroscopic defects, being the origin of the

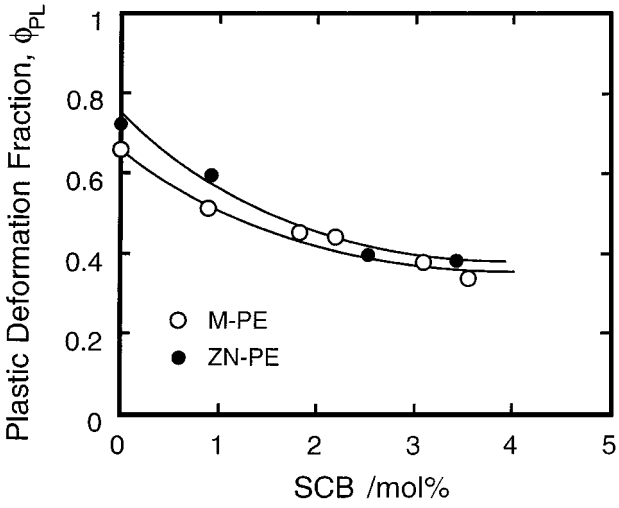

Figure 5 Plastic strain fraction $\phi_{PL}(t)$ at an applied strain of 0.16 plotted against short-chain branching for (○)metallocene-catalyzed PEs and (●) Ziegler-Natta-catalyzed PEs.

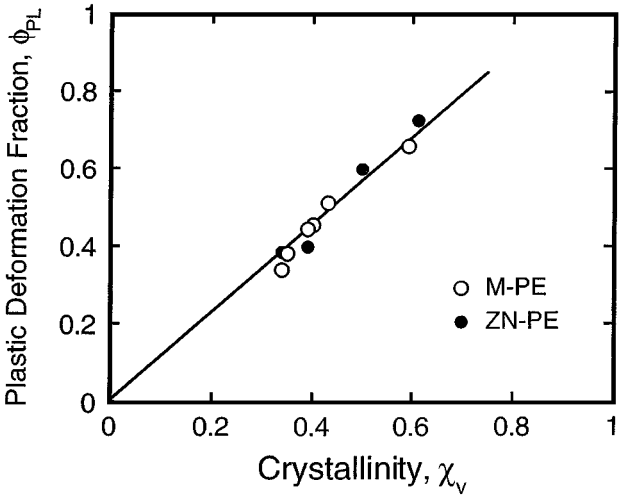

Figure 6 Plastic deformation fraction $\phi_{PL}(t)$ at an applied strain of 0.16 plotted against the degree of crystallinity in volume fraction for (○) metallocene-catalyzed PEs and (●) Ziegler-Natta-catalyzed PEs.

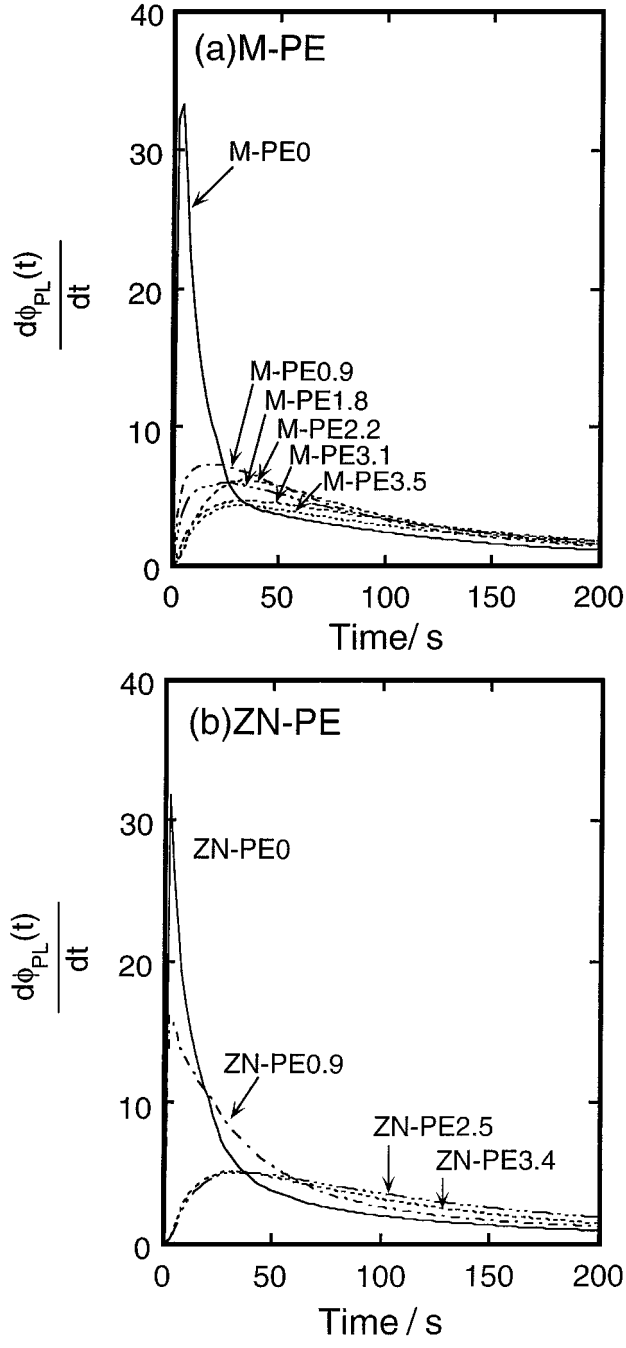

Figure 7 Derivative curves of $\phi_{PL}(t)$ for (a) metallocene-catalyzed PEs and (b) Ziegler-Natta-catalyzed PEs.

stress-whitening in the higher strain region. Indeed, this has already been demonstrated from our previous ultrasonic measurements for other polyethylenes and polypropylenes [38, 39].

As is also seen in Fig. 7, the plastic deformation behaviour of ZN-PE0.9 differs significantly from that of other branched PE samples and has similar behaviour to M-PE0 and ZN-PE0. Considering that the ZN-PE0.9 sample has heterogeneous SCB distribution and a lower SCB content, the comonomer units should be excluded from crystals when a molecule crystallizes. Therefore, it follows that the molecular organization of its crystalline phase, which is a key factor in plastic deformation, is similar to that of unbranched PE, *i.e.* M-PE0 and ZN-PE0.

4.2. Anharmonicity

The crystallinity dependence of the Grüneisen constant γ_G is shown in Fig. 8. The figure shows that the values of γ_G are between 1 and 4, which are comparable to the published data of typical polyethylene materials [40, 41]. It is of significant interest to note that M-PEs exhibit a linear relationship between γ_G and crystallinity, and the data extrapolate to the origin for zero crystallinity. Thus, a completely amorphous polymer is suggested to display no anharmonic response. Considering that the decrease in crystallinity for M-PEs is caused not by the increase in the amorphous layer but by the decrease in the crystalline thickness, the increase in crystallinity causes a greater strain to be imposed on the amorphous parts in the initial deformed states, which can lead to a higher nonlinearity in elastic response. It should be noted here that the γ_G values of branched ZN-PEs are lower that those of M-PEs at the same crystallinity. This seems to be associated with the differences in microstructures between M-PE and ZN-PE.

In general, the materials with a higher degree of crystallinity show stronger anharmonicity whilst the rubberlike ones show a harmonic response. In

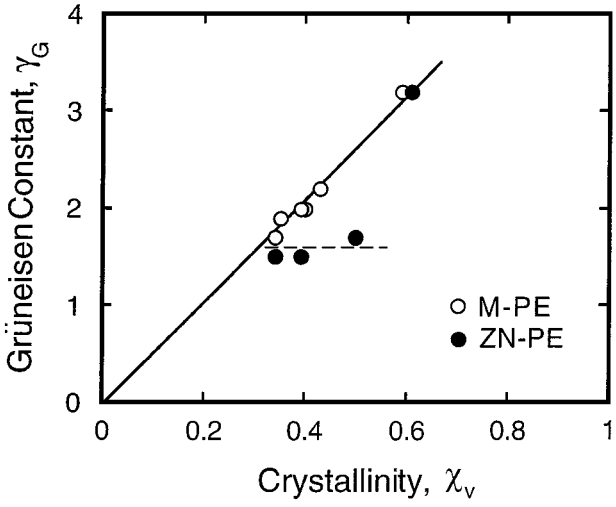

Figure 8 Relationship between the Grüneisen constant γ_G and the degree of crystallinity in volume fraction for (○) metallocene-catalyzed PEs and (●) Ziegler-Natta-catalyzed PEs.

addition, in contrast to the plastic deformation, the degree of anharmonicity seems to be affected mainly by the soft components of the materials because the anharmonic response is effectively enhanced by a large deformation. The heterogeneous incorporation of comonomer units along a main chain in branched ZN-PEs leads to an increase of amorphous thickness rather than a decrease of lamellar thickness as well as to broader distributions in the crystalline thickness. At the beginning of deformation, the less-organized crystalline portions with a higher amorphous fraction act as strain concentrators because of their lower modulus. Consequently, the fact that the branched ZN-PEs exhibit a lower γ_G seems to be attributed to the strain concentration on the soft component.

4.3. Stress-relaxation behaviour

The nonlinear parameters such as the degrees of plasticity and of anharmonicity in Equation 8 were found to

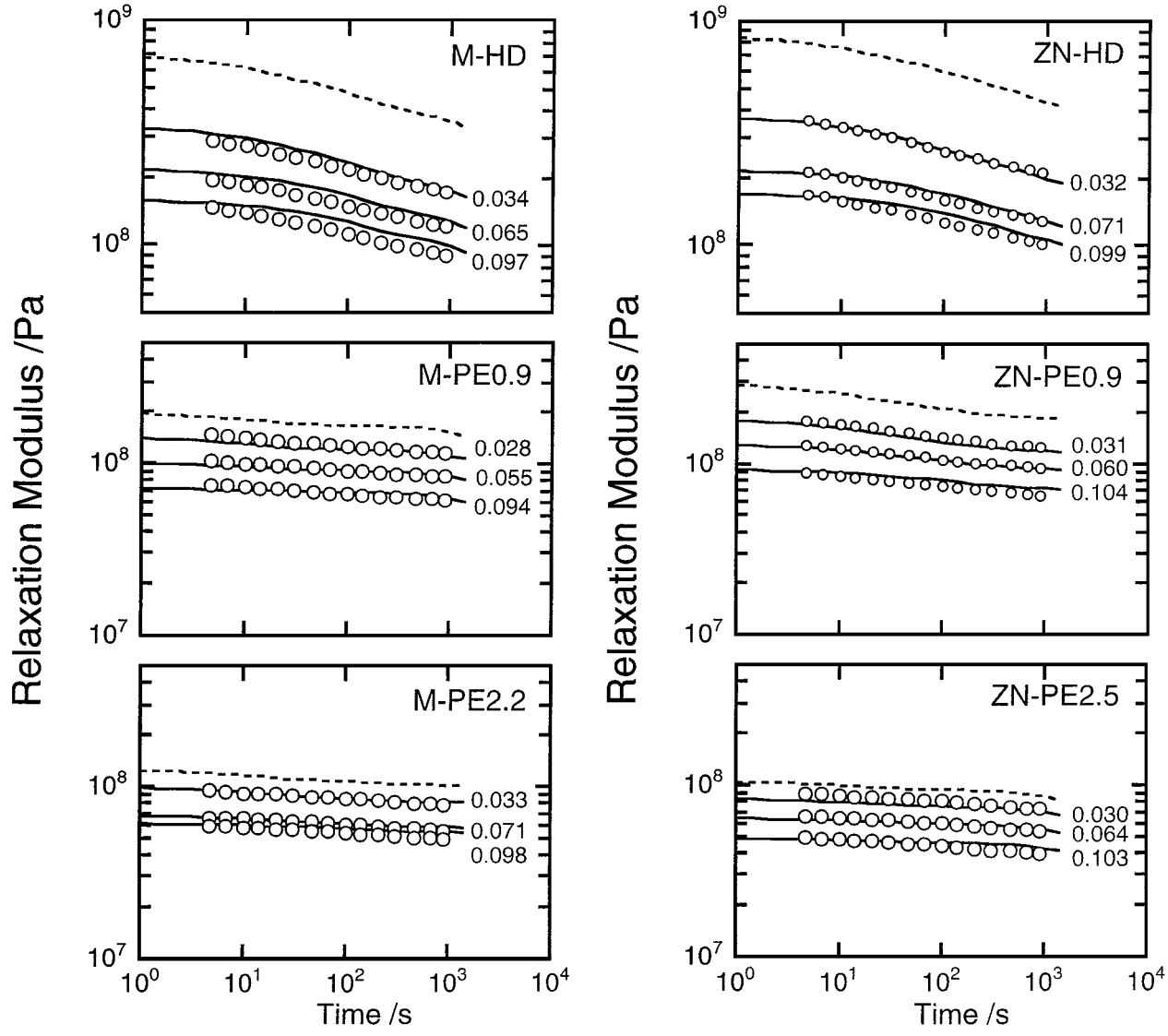

Figure 9 Relaxation modulus under various natural strain levels for Ziegler-Natta-catalyzed PEs and metallocene-catalyzed PEs. The solid lines denote the theoretical values, the dotted lines denote the values predicted from the linear viscoelastic theory, and the open circles denote experimental values.

be evaluated by experimental data obtained from simultaneous measurement of elongation and oscillatory deformation. We can develop the constitutive Equation 8 to predict the stress-relaxation behaviour in the nonlinear region. The model predictions were then compared with the experimental results, in order to confirm the validity in these nonlinear parameters.

Stress-relaxation tests of 10^3 s duration were conducted using the dynamic mechanical analyzer at natural strain levels up to about 10% in which all the samples were in the pre-yield region. The initial length between clamps was 20 mm and the temperature was kept at 298 K during the experiment. The loading process was to ramp at a constant deformation rate of 1.0 mm/min to the desired strain levels.

The stress-relaxation behaviour can be obtained as [42]

$$\sigma(\theta) = \int_{-\infty}^{\infty} \left\{ \int_{0}^{t_0} \exp\left(-\frac{t_0 - t'}{\tau} \right) \Gamma(\varepsilon) \frac{R}{1 + Rt'} \times \Psi(t')\, \mathrm{d}t' \right\} H(\tau) \exp\left(-\frac{\theta}{\tau} \right) \mathrm{d}\ln\tau \qquad (18)$$

where t_0 is the time after a ramp process. Putting the experimental data; *i.e.* the Grüneisen constant γ_G, the effective strain fraction $\Psi(t)$ and the linear relaxation modulus $E(t)$, into Equation 18 provides the stress-relaxation behaviour. The relaxation modulus in the nonlinear region defined in this work by $\sigma(\theta)/\gamma_0 = \sigma(\theta)/\ln(1 + Rt_0)$, where γ_0 is the applied natural strain, was compared with the experimental results, as exemplified in Fig. 9, The theoretical predictions are in excellent agreement for all the samples. In the figures, the computational results from the linear viscoelastic theory are also included as dotted lines. A comparison with the predictions from the linear viscoelastic model demonstrates that the present nonlinear model succeeded in describing vertical shifting of the linear stress-relaxation behavior in the nonlinear regions. The vertical shift seems to be attributed mainly to the reduction in elastic modulus due to the anharmonicity of the materials.

5. Conclusions

The nonlinear tensile behaviour in the pre-yield region for two sets of linear butyl-branched polyethylenes prepared using metallocene and Ziegler-Natta catalysts was investigated using a nonlinear constitutive equation in which the plastic deformation and the anharmonicity of elastic response are taken into account. The important conclusion concerning the mechanical behavioural difference between both polyethylenes is that the branched Ziegler-Natta-catalyzed polyethylenes show a higher degree of the plastic deformation and that the branched metallocene-catalyzed polyethylenes show a higher anharmonicity when the polyethylenes of almost the same SCB content are compared. Considering that the plastic deformation fraction depends largely on the hard components (well-organized crystalline regions) whilst the anharmonicity is governed by the stress response from the soft components (less-organized crystalline regions), the differences in mechanical nature between both branched polyethylenes arise from the differences in microstructures between metallocene-catalyzed and Ziegler-Natta catalyzed polyethylenes.

Furthermore, it was found that the nonlinear parameters such as ϕ_{PL} and γ_G obtained from the stress-strain responses enable us to predict the stress-relaxation process of polyethylenes in the nonlinear region. The authors emphasize that the present experimental and analytical techniques become a great help in the quantitative characterization of the effects of microstructures and/or molecular morphology on the mechanical properties for semicrystalline polymers. Thus, these mechanical parameters obtained by the present method will be fundamental in design and application of polyethylene materials.

References

1. C. ZHANG and I. D. MOORE, *Polym. Eng. Sci.* **37** (1997) 404.
2. C. F. POPELAR, C. H. POPELAR and V. H. KENNER, *ibid.* **30** (1990) 577.
3. R. S. LAMOND, "Plastic Pipes, Vol. 1" (Edinburgh, UK, 1995) p. 1.
4. C. ZHANG and I. D. MOORE, *Polym. Eng. Sci.* **37** (1997) 414.
5. I. M. WARD and P. W. HADLEY, "An Introduction to the Mechanical Properties of Solid Polymers" (Wiley, New York, 1996).
6. J. LAI and A. BAKKER, *Polym. Eng. Sci.* **35** (1995) 1339.
7. R. S. BRETZLAFF and R. P. WOOL, *J. Appl. Phys.* **52** (1981) 5964.
8. Y. WADA, A. TANAI, T. NISHI and S. NAGAI, *J. Polym. Sci. A-2* **7** (1969) 201.
9. L. LIN and A. S. ARGON, *J. Mater. Sci.* **29** (1994) 294.
10. R. J. SAMUELS, in "Plastic Deformation of Polymers," edited by A. Peterlin (Marcel Dekker, New York, 1971) p. 241.
11. P. B. BOWDEN and R. J. YOUNG, *J. Mater. Sci.* **9** (1974) 2034.
12. K. NITTA and M. YAMAGUCHI, *ibid.* **33** (1998) 1015.
13. J. G. FATOU, I. G. MACIÁ, C. MARCO, M. A. GÓMEZ, J. M. ARRIBAS, A. FONTECHA, M. AROCA and M. C. MARITÍNEZ, *ibid.* **31** (1996) 3095.
14. A. J. PEACOCK and L. MANDELKERN, *J. Polym. Sci., Polym. Phys.* **28** (1990) 1917.
15. L. MANDELKERN, *Polymer J.* **17** (1985) 337.
16. S. HOSODA and A. VERMURER, *ibid.* **29** (1992) 939.
17. G. CAPACCIO and I. M. WARD, *J. Polym. Sci., Polym. Phys.* **22** (1984) 475.
18. K. SHIRAYAMA, T. OKADA and S. KITA, *J. Polym. Sci.* **A3** (1965) 907.
19. S. HOSODA, *Polymer J.* **20** (1988) 383.
20. L. WILD, T. R. RYLE, D. C. KNOBELOCH and I. R. PEAT, *J. Polym. Sci., Polym. Phys.* **20** (1982) 441.
21. W. KAMMINSKY, H. HAHNSEN, K. KÜLPER and R. WÖLDT, U. S. Patent no. 4, 542, 199 (1985).
22. K. HEILAND and W. KAMMINSKY, *Makromol Chem.* **193** (1992) 106.
23. T. UOZUMI and K. SOGA, *ibid.* **193** (1992) 823.
24. N. W. TSCHOEGL, "The Phenomenological Theory of Linear Viscoelastic Behavior An Introduction" (Springer–Verlag, Berlin, 1989).
25. M. TODA, *J. Phys. Soc. Japan* **22** (1961) 431.
26. T. G. GIBBONS, *Phys. Rev.* **B7** (1973) 1410.
27. K. NITTA, Y. UCHIDA and A. TANAKA, *Polymer J.* **23** (1991) 895.
28. S. ONOGI, A. TANAKA and M. ISHIKAWA, *ibid.* **7** (1975) 467.
29. A. TANAKA, K. TANAI and S. ONOGI, *Bull. Inst. Chem. Res. Kyoto Univ.* **55** (1977) 177.
30. T. YAMAGUCHI, T. YANAGAWA and S. KIMURA, *Sen-i Gakkaishi* **32** (1976) 403.

31. G. W. BECKER and H. J. RADEMACHER, *J. Polym. Sci.* **58** (1962) 621.
32. J. C. RANDALL, *J. Polym. Sci., Polym. Phys.* **11** (1973) 275.
33. E. T. HSIEH and J. C. RANDALL, *Macromolecules* **15** (1982) 1402.
34. K. NITTA, K. SUZUKI, S. NOJIMA and A. TANAKA, *Recent Res. Dev. Polym. Sci.* **3** (1999) 143.
35. R. CHIANG and P. J. FLORY, *J. Amer. Chem. Soc.* **83** (1961) 2057.
36. F. R. SCHWARZL, *Rheol. Acta* **14** (1975) 581.
37. A. V. TOBOLSKY and K. MURAKAMI, *J. Polym. Sci.* **40** (1959) 443.
38. A. TANAKA and K. NITTA, *Polym. Eng. and Sci.* **31** (1991) 571.
39. M. YAMAGUCHI and K. NITTA, *ibid.* **39** (1999) 833.
40. B. K. SHARMA, *Polymer* **24** (1983) 314.
41. E. L. RODRIGUEZ and F. E. FILISKO, *J. Mater. Sci.* **22** (1987) 1934.
42. K. NITTA and K. SUZUKI, *Macromol. Theory and Simul.* **8** (1999) 254.

Received 12 May
and accepted 21 October 1999